IN SILICO STRUCTURAL ANALYSIS OF THE COMPLEX BRI1 RECEPTOR LIKE KINASE, PAMP BRASSINOLIDE AND SERk1 CO-RECEPTOR

By

Mehnaz Nafisa Naurin
16136020

A thesis submitted to the Department of Mathematics and Natural Sciences in partial fulfillment of the requirements for the degree of
Bachelor of Science in Biotechnology

Mathematics and Natural Sciences
Brac University
April 2021

Declaration

It is hereby declared that

1. The thesis submitted is my own original work while completing degree at Brac University.
2. The thesis does not contain material previously published or written by a third party, except where this is appropriately cited through full and accurate referencing.
3. The thesis does not contain material which has been accepted, or submitted, for any other degree or diploma at a university or other institution.
4. I have acknowledged all main sources of help.

Student's Full Name & Signature:

Mehnaz Nafisa Naurin
16136020

Approval

The thesis titled “In silico structural analysis of the complex BRI1 receptor like kinase, PAMP Brassinolide and SERk1 co-receptor” submitted by Mehnaz Nafisa Naurin (16136020) of Spring, 2021 has been accepted as satisfactory in partial fulfillment of the requirement for the degree of Bachelor of Science on 2021.

Examining Committee:

Supervisor:
(Member)

_____

M H M Mubassir
Lecturer, Biotechnology Program
Department of Mathematics and Natural Sciences

Program Coordinator:
(Member)

_____

Iftekhar Bin Naser, PhD
Assistant Professor
Department of Mathematics and Natural Sciences

Departmental Head:
(Chair)

_____

Prof. Dr. A F M Yusuf Haider
Professor and Chairperson
Department of Mathematics and Natural Sciences

Ethics Statement

Hereby, I Mehnaz Nafisa Naurin consciously assure that for the manuscript "In silico analysis of structural complex of BRI1 receptor like kinase, PAMP Brassinolide and SERk1 co-receptor" the following is fulfilled:

1) This material is the authors' own original work, which has not been previously published elsewhere.

2) The paper reflects the authors' own research and analysis in a truthful and complete manner.

3) The paper properly credits the meaningful contributions of co-authors and co-researchers.

4) The results are appropriately placed in the context of prior and existing research.

5) All sources used are properly disclosed (correct citation).

6) All authors have been personally and actively involved in substantial work leading to the paper, and will take public responsibility for its content.

I agree with the above statements and declare that this submission follows the policies of the ethical statement.

Student's Full Name & Signature:

Mehnaz Nafisa Naurin
16136020

Abstract

Plants that are sessile species are constantly associated with exposure to pathogenic organisms abundant in their biosphere. Comprehending the hypothesis next to it would be a significant attempt to study the processes to prevent diseases in plants. In the process, a typical function of plant-innate immune responses is the identification of disease-causing organisms by pattern recognition receptors (PRRs). In plants defense system kinase complexes facilitate PRR signaling at the cell surface, leading to the stimulation of immunological processes which just treat and prevent the pathogenic invasion. Here, in certain steps, the BRI1-BLD-SERk1(PDB ID: 4lsx) complex crystallographic structure was designed to simulate for 5ns, as five distinct collaboration of the core crystallographic structure were included. 5ns simulation model projections were then reviewed for each arrangement in order to acquire a preview of the connection as well as immune susceptibility of BRI1 against BLD with the significant help of co-receptor SERk1. In this analysis, BRI1-BLD-SERK1 complex clearly shows how BLD operates as a "molecular glue" which facilitates the receptor's interaction with its co-receptor, which may induce their kinase domains to attach and thereby stimulate the signaling pathway. The crystal configuration of BRI1-BLD-SERK1 complex further shows that the binding region for BLD is formed by LRRs 21-25 and together with the island domain. In addition, it was found that hydrogen-bonding interactions with tyrosine residues in the BRI1 island domain are formed by BLD. So, any transformation to such BLD attached areas can thus be considered to be significantly catastrophic to the plant, leading to the inability of the PRR to trace the PAMP. Since BRI1 has been shown to make a significant contribution in *Arabidopsis thaliana*'s plant defense system, its hypothesized binding procedure with the BLD and co-receptor SERk1 will help us to construct a better overview of the initiation phase of PTI.

Dedication

Acknowledgement

I would like to express my special thanks of gratitude to my supervisor **M H M Mubassir** who gave me the golden opportunity to do this wonderful project on the topic "In silico analysis of structural complex of BRI1 receptor like kinase, PAMP Brassinolide and SERk1 co-receptor", which also helped me in doing a lot of research and I came to know about so many new things.

I would also like to extend my sense of obligation to **Prof. A F M Yusuf Haider**, Ph.D. Chairperson, Department of Mathematics and Natural Sciences, BRAC University, Iftekhar **Bin Naser, PhD** program Coordinator, Department of Mathematics and Natural Sciences, BRAC University, for allowing me to pursue my research in the field of my interest.

Lastly, I am are overwhelmed in all humbleness and gratefulness to acknowledge my depth to all those who have helped me to put these ideas, well above the level of simplicity and into something concrete.

Table of Contents

List of Tables

List of Figures

List of Acronyms

AA	**Amino Acid**
ETI	Effector Triggered Immunity
GROMACS	Groningen Machine for Chemical Simulations
H-bonds	Hydrogen Bonds
LRR	Leucine Rich Repeat Domain
MD	Molecular Dynamics
PAMP	Pathogen Associated Molecular Pattern
PDB	Protein Data Bank
PRR	Pattern Recognition Receptor
PRR-RKs	Pattern Recognition Receptor like kinases
PTI	Pattern Triggered Immunity
Rg	Radius of Gyration
RMSD	Root Means Square Deviation
RMSF	Root Means Square Fluctuations

List of Symbols

Aº	Angstrom
K	Kelvin
nm	Nano meter
ns	Nano second
ps	Pico second

Chapter 1

Introduction

1.1Background Study

There is a range of ways for plants to protect themselves against pathogens. The plant immune system's commonly used model is divided into a general response triggered by pathogen-associated molecular patterns (PAMPs) and a specific reaction triggered by the effectors. The first type of response is recognized as PAMP triggered immunity (PTI), and the second type is defined as effector-triggered immunity (ETI). [1]

The vibrant receptive reflection of pathogen or microbe associated molecular patterns through pattern recognition receptors on the plant's cellular surface is the first of these functions. To give an example, Pattern recognition receptors (PRR) 'FLS2 (flagellin sensitive 2),' a leucine-rich repeat receptor kinase (LRR-RK) placed inside the plasma membrane, assist plants in infiltrating bacterial flagellin.

Effector Triggered Immunity (ETI) is a plant immune response system in which intracellular immune sensors are added, approximately all of which are leucine-rich repeat (NBS-LRR) nucleotide-binding site proteins, which are configured to identify harmful effectors conveyed explicitly or implicitly.

1.2 Research aims and objectives

The primary goal of this study is to better understand pattern triggered immunity (PTI) in *Arabidopsis thaliana*. More concretely,

- To study the interaction between PRR BRI1, PAMP BLD, and Coreceptor SERK1by using Molecular Dynamic (MD) Simulation.
- Involvement of the co-receptor SERK1 and PAMP BLD in PTI of ***Arabidopsis thaliana.***

1.3 Literature review

In this segment, the fundamentals of pattern triggered immunity are covered, and also the model plant and its morphology. Few terminologies are also discussed in relation to pattern triggered immunity. Computational methods and terminology understanding are also assessed at the bottom of this part.

1.3.1 Arabidopsis thaliana

The revolution of the 1980s in plant biological science, molecular genetics, and physiology cemented Arabidopsis' position as a model plant. Around the time, there were many other plans for prototypes obtained from plants, like petunia being recommended because of its transition stability as well as scarcity of haploid lines, and tomatoes being preferred for mutant functionality. Similarly, in 1975, George Re'dei offered Arabidopsis as a model plant for the finding of auxotrophic mutation, and then it was later demonstrated in an article that was published in the Annual Review of Genetics, drawing the enthusiasm of both molecule cloners and aspiring geneticists.

Arabidopsis thaliana is a small herb within the mustard family; for more than 80 years, it has been a convenient topic for research into classical genetics [1, 2]. Researchers have recently

recognized that this flowering plant also has a genome size and genomic organization that recommends it for molecular genetics' experiments [3,4,5]. Due to the comfort with which this plant functions in classical and molecular genetics, Arabidopsis is commonly used in plants as a model organism for examining genetics, growth, physiologies and biochemistry of molecular disease. [6]

The lifecycle of *Arabidopsis thaliana* takes approximately six weeks to finish, which include seed germination, rosette growth, stems and branches bolting, flowering, as well as preliminary seed growth. In the self-pollination phase due to uncovered bud, pollen can indeed be relocated to the stigma outer for crossing until it attains a scale of 2 mm flower in size and shape, which is quite tiny.

1.3.2 Pattern Triggered Immunity (PTI)

Pattern triggered immunity (PTI) is the very first way of responding of the plant immune system, that is stimulated by the signal of microbe or pathogen associated molecular patterns (MAMPs or PAMPs) by pattern recognition receptors (PRRs). Integrated pathogens have obtained effector proteins for repressing PTI, which is often delivered to the plant cell through evolution. At the time of invasion MAMPs (Microbe-Associated Molecular Patterns) and DAMPs (damage Associated Molecular Patterns) derived from the host, triggering the release of a multitude of pathogens. Pattern Recognition Receptors (PRRs) on the cell surface assist to identify pathogenic agents, then these PRRs facilitate PTI for the immune function sensitivity.

PTI is able to effectively pull off a variety of microorganisms due to the conserved nature of PAMPs. As a matter of fact, basal immunity evolves all through the infection. PTI has a versatile and restrained immune system response to the multitude of non-host microorganisms.

1.3.3 Effector Triggered Immunity (ETI)

Another plant immune system, widely recognized as effector-triggered immunity (ETI), is likely to focus on order to detect effectors via peripheral receptors. These receptors are produced mostly during coevolutionary phase. In ETI, a Resistance (R) gene product targets the pathogen's effector protein(s) inside the plant cell. Usually all of the R genes are observed in nucleotide-binding leucine-rich repeat (NB-LRR) proteins. Once these NB-LRR proteins

sense an effector, ETI tends to start. This strategy used by NB-LRR to categorize effectors is based on the findings of their actions.

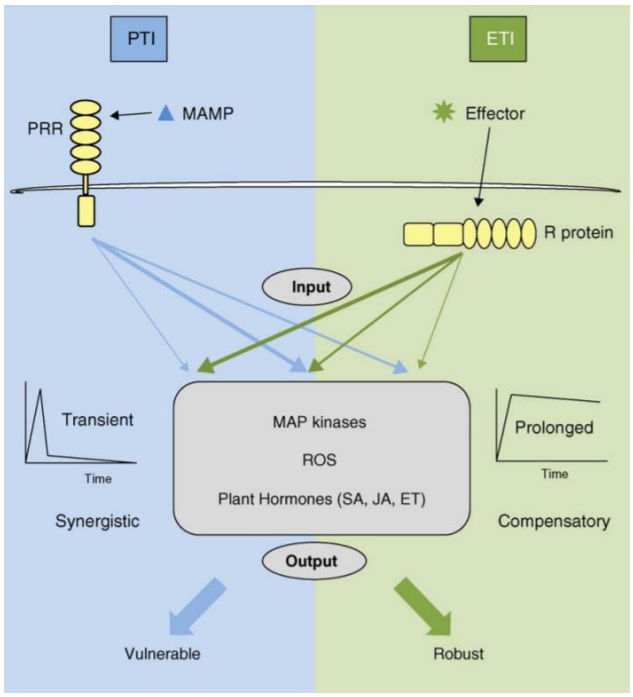

Fig 1.1: Signaling differences between PTI and ETI.

1.3.4 Complexes

A significant group of phytohormones, which affect a wide variety of physiological mechanisms essential for plants' growth and development, are brassinosteroids (BRs) [39]. BR signaling complications exhibit numerous deficits, like dwarfism, flowering slowdown, decreased seedling growth, low fertility ratios, as well as inappropriate stomatal distribution. [40] Brassinosteroid insensitive 1 (BRI1), a receptor kinase located on the cellular surface, actually begins the BR signaling. BRs are detected by the extracellular domain of BRI1, contributing to heterodimerization with the co-receptor somatic embryogenesis receptor kinase (SERK). This is accompanied by the BRI1 and SERK1 intracellular kinase domains' transphosphorylation, prompting a downstream signaling mechanism. Ultimately leads to major genes being activated or inhibited. [40-44] The significant challenge in the BR signaling is the recognition of BRs via the BRI1 receptor. [45]

Besides, the BRI1 receptor (Brassinosteroid) offers a model for understanding receptor-mediated signaling in plants. [7].

Membrane-integral receptor kinases are found in plants that detect various extracellular signals, such as steroid hormones [9], peptides [10], and proteins [11]. The steroid receptor kinase BRI1, which regulates the growth and development of plants [12], binds to its LRR ectodomain [13-16], the hormone brassinolide (BLD). BLD binding to BRI1 causes the ordering of a ~70-residue island domain which, together with the LRR centre, can form a docking platform for a co-receptor protein [15, 16]. The size of the contact surface envisaged and its proximity to the membrane indicates that there are possibly co-receptor candidates for the SERK family of plant receptor kinases. [17-20]

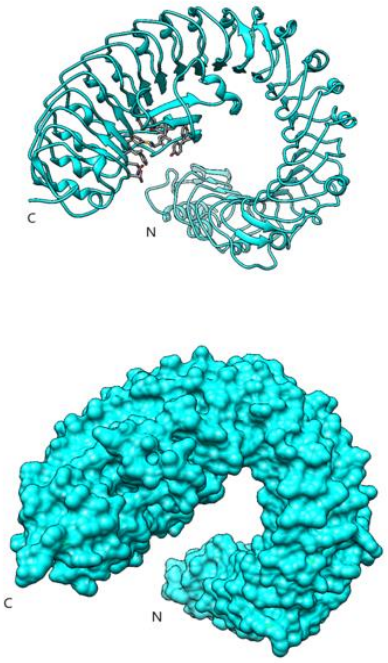

Fig1.3.4 (A): Illustration of BRI1 LRR

Furthermore, Throughout the plant cellular membranes, BRI1 is situated that comprising of an extracellular ligand-binding region, a single transmembrane helix, and also an intracellular serine/threonine bound kinase domain. There are 25 leucine-rich repeats (LRRs) inside this extracellular domain as well as a right-handed superhelical design is hypothesized. [46,47] The inclusion of an island domain, that involve those 70 amino acid residues among LRRs 21 and 22, is indeed a remarkable aspect of this region of the receptor [46, 48].

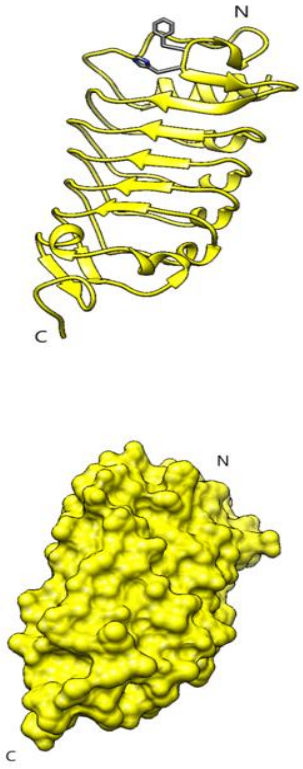

Fig1.3.4 (B): Co-receptor SERk1's surface and cartoon structural representation

In the plasma membrane of protoplasts, the interaction between BRI1 and SERK1 takes place. Besides that, we already know, there have been approximately 600 genes coding for receptor-like kinases in Arabidopsis (*Arabidopsis thaliana*). A comparatively tiny proportion of these RLKs are confined for practical aspects; BRI1 receptor helps SERK1 to form heterodimers, which clearly indicates that the co-receptor has comparable performance concerning the BRI1 signaling and/or internalization. [49] Moreover, the co-receptor SERK1 is recruited to stimulate brassinosteroid associated signaling. The previous research also reveals how the interaction of serk1 and BRI1 influences BRI1-mediated signaling in planta. The inclusion of five LRRs, including canonical N- and C-terminal capping motifs obtained from plant LRR proteins was identified by the 1.5 Å crystal structure of SERK1. As it is already observed that the transformation of complexes is BL-dependent which means that the hormone itself mediates the initial physical connection of the ectodomain BRI1 and SERK1.

Further, also the wild-type BRI1 ectodomain could be used to generate related complexes. In the development of the BRI1-SERK1 complex, LRR capping domains are actively engaged: The N terminal cap of SERK1 creates folding's on the upper part of the BRI1 steroid attaching region. It develops interactions with the island domain of BRI1, including BRI1 LRR 25 (726 to 729 residues of BRI1) and the hormone component. SERK1 residue Phe61 (which tends to be disordered in the independent design of SERK1) develops a stacking contact with the hormone's C ring, whereas the adjacent histidine (His62) develops hydrogen bonds with brassinolide's (BLD) 2a,3a-diol moiety. Moreover, by forming interactions with residues derived directly from SERK1 LRRs, the C-terminal cap of BRI1 participates in complex construction. The SERK1 residues Tyr97, Tyr101, Tyr125 and Phe145 and residue Met745 in the BRI1 C-terminal cap have significant nonpolar correlations. In the complex formation after the binding of BLD, the island domain is gradually organized, allowing the receptor to activate. When BLD is connected to BRI1, BLD's A-D rings are aligned in between LRR center point

and the island domain in a hydrophobic groove, whilst the alkyl chain moves into some kind of narrow pocket developed by LRRs 21 and 22 as well as the island domain.

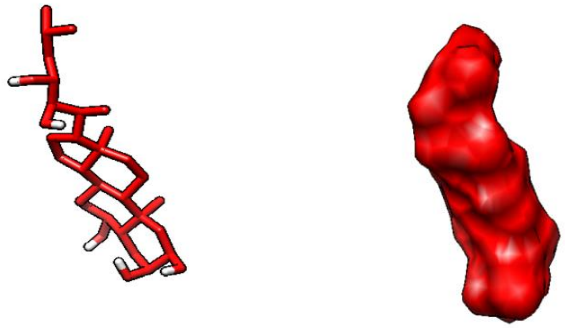

Fig1.3.4 (C): Cartoon and surface structural view of Brassinolide (BLD)

It has already been determined that BLD connections with both the island domain residues and the LRR core are likely to be crucial for BLD binding. Mutations have been identified within the residues of the island domain including surrounding LRRs, adversely influencing the BLD linking and ultimately the downstream signaling. The island domain, similarly the adjacent LRR core are therefore vital for BLD perception. Prior studies have listed BLD as the most bioactive BR. Structurally, it is a steroid with a distinct lactone group within its B-ring, including vicinal diols in both its A-ring and alkyl chain. In the BR I1-BLD formation, there are mainly two pathways followed by it. BLD is expected to enter the BRI1 binding pocket in the first pathway for BLD attachment with its fused A-D rings surrounding the binding region.

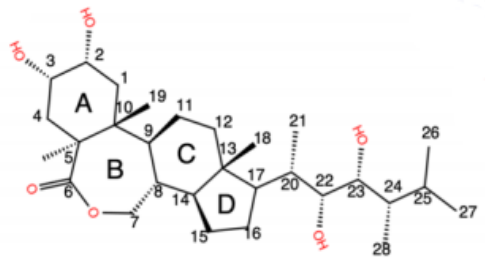

Fig1.3.4 (D): Chemical structures of Brassinolide (BLD)

Then it continues even further into the pocket to engage with S647 of the BRI1 island domain through its hydroxyl group in the A-ring C2. After that, the hormone rings seem to be heading away from the pocket that binds. This may be a feature of the flipping procedure, whereby BLD reverses alignment to permits the pocket to enroll its side chain and eventually make the assumption of binding position. During this stage, it still retains the prior linkage with S647, yet through the two oxygens in its B-ring, it establishes latest contact with T649. The second

binding trajectory followed by BLD differs with the previous one in the way that the side chain of the ligand now directs it into the binding pocket rather than the fused rings of BLD. The hydroxyl groups of C22 and C23 of the side chain connect to S647 during this first phase, however, BLD has still not reached the BRI1 attaching region. BLD reaches the binding pocket afterwards, yet still not in its binding mode. The prior contact with S647 persists, thus establishing new interactions with Y642 and N705 via the oxygen of the ring and its B ring's carbonyl oxygen accordingly. Then, BLD eventually binds to the BRI1 receptor.

1.3.5 Computation approach for Molecular Dynamic (MD) simulation

Molecular dynamics (MD) is a methodology for computer simulation to test the physical motion of atoms and molecules. The atoms and molecules are approved to engage for a stiff period of time to observe the dynamic "evolution" of the system. In the common version, the trajectories of atoms and molecules are protected by numerically resolving Newton's motion equations for the interactive particles system, where the forces between the particles and their potential energies are often analyzed using interatomic potentials or molecular mechanics force fields. The procedure is majorly applied in the fields of chemical physics, materials science and biophysics. As molecular systems typically consist of a large number of particles, it is not possible to analytically determine the characteristics of such complicated systems; MD simulation uses computational techniques to circumvent this problem. Long MD simulations, however, are mathematically ill-conditioned, producing cumulative errors in numerical integration that can be minimized but not completely removed with the correct assortment of algorithms and parameters. [21]

1.3.6 Protein-Ligand Interaction Profiler (PLIP)

The portrayal of interactions in protein–ligand complexes is vital for research in structural bioinformatics, drug discovery and biology. nevertheless, comprehensive tools are not voluntarily accessible to the research community. Here, we introduce the protein–ligand interaction profiler (PLIP), a novel web service for fully automated detection and visualisation of relevant non-covalent protein–ligand contacts in 3D structures, openly accessible at PLIP

site. The input is either one Protein Data Bank structure, one protein or ligand name, or a custom protein–ligand complex (e.g., from docking). In compare to other tools, the rule-based PLIP algorithm does not need any structure formulation. It proceeds a list of discovered interactions on single atom level, covered by seven interaction types (hydrogen bonds, hydrophobic contacts, pi-stacking, pi-cation interactions, salt bridges, water bridges and halogen bonds). PLIP stands out by oblation publication-ready images, PyMOL session files to produce routine images and parsable result files to facilitate successive data processing. The full python source code is ready for download on the website. PLIP's command-line mode allows for high-throughput contact profiling. [22]

1.3.7 Protein Interactions Calculator (PIC)

Interactions within a protein structure and interactions among proteins in an arrangement are critical factors in describing the stability and functional molecular basis of proteins and their complexes. There are many weak and powerful interactions that provide a protein structure or an assembly with stability. The Protein Interactions Calculator (PIC) is a server that measures different interactions, including disulphide bonds, interactions within hydrophobic residues, ionic interactions, hydrogen bonds, aromatic-aromatic interactions, aromatic-sulphur interactions, and cation-pi interactions among a protein or between proteins in a complex collection of 3D structures of a protein or assembly. [23]

1.3.8 MM-PBSA

The molecular mechanics energies joint with the Poisson–Boltzmann or generalized Born and surface area continuum solvation (MM/PBSA) methods are common approaches to estimate the free energy of the binding of small ligands to biological macromolecules. They are usually based on molecular dynamics mockups of the receptor–ligand complex and are therefore transitional in both accuracy and computational endeavor between empirical scoring and strict alchemical perturbation methods. They have been used to a large number of systems with varying success. MM/PBSA methods are attractive approaches owing to their modular nature and that they do not necessitate calculations on a training set. They have been used magnificently to reproduce and rationalize experimental findings and to improve the results of simulated screening and docking. However, they contain several crude and questionable

approximations, for example, the lack of conformational entropy and information about the number and free energy of water molecules in the binding site. Moreover, there are many variants of the method and their performance varies strongly with the tested system. Likewise, most attempts to ameliorate the methods with more accurate approaches, for example, quantum-mechanical calculations, polarizable force fields or improved solvation have deteriorated the results. [24]

1.3.9 Solvent accessible surface area (SASA)

Solvent accessible surface area (SASA) of proteins has always been considered as a decisive factor in protein folding and stability studies. It is defined as the surface characterized around a protein by a hypothetical center of a solvent sphere with the van der Waals contact surface of the molecule. The measurement of a bulk region alone is not sufficient for additional studies, so alternative procedures have been established. Without moving the van der Waals surface of the atoms accessible to the contact surface, a network of hollow and saddle-shaped surfaces forms a bond on that process. [25-27] The technique has recently been advanced again to solve a minor problem. If the probe sphere is precluded and not to withstand the intersection of van der Waals, then how can SASA of that molecule be calculated? By improving algorithms for the measurement of touch and transition surfaces, as well as for the accessible solvent region that helps measure SASA of any molecules. [28-30]

1.3.10 Hydrogen Bond

The hydrogen bond is the most essential interatomic exchange in protein folding. (31,32) However, when mediocre intermolecular hydrogen bond energy is very medium compared to covalent bond, their enormous amount of presence gives a crucial influence on protein folding at another stage, the folding process prevails, but their role is primarily reserved for hydrophobic interaction [31-34]. The vast majority of protein hydrogen bonds are main chains of NH to CO bonds and mainchain and side-chain bonds create a flock the caps of helices close by. It is very rare for main-chain NH or CO clusters to collapse to create hydrogen bonds.[32]

Chapter 2

Materials and Methods

The procedures followed to evaluate the interaction between BRI1-Brassinolide-SERK1 are defined in this section. Various kinds of open-source computing software and servers have been used for research. MM-PBSA, RCSB Protein Data Bank, Protein-Ligand Interaction Profiler (PLIP), Protein Interactions Calculator (PIC), XmGrace, Chimera and so on, which are GROMACS version in the 2018.x series. For the open-source platform, all the software is developed and the testing processes are carried out for running on the Linux-based Ubuntu system.

2.1 Molecular dynamic simulation of BRI1 PRR, PAMP Brassinolide and Co-Receptor SERk1

At an early stage, the first protein to combine the ectodomain BRI1 receptor with PAMP Brassinolide and Co-Receptor SERk1 (PDB code: 4lsx) was obtained from the web server of the Protein Data Bank. The file was downloaded using the format '.pdb'. In a text editor, the PDB file was published and edited by keeping all the protein residues inside. After saving the file, PIC data was collected in accordance with the search category for protein-protein interaction. The PDB file was later sent to the GROMACS software suite for molecular dynamic (MD) simulation.[35] For this simulation, GROMOS 54a7 unified force field was preferred, much like a force field. The system was solved, neutralized, subsequently minimized and balanced by electricity. The protein complex was applied to a dodecahedron box with a minimum distance of 1Å ranging from the protein surface to the edges during solvation. The newly formed box with the inward protein complex was solved with the SPC water model.[36] The device was neutralized with the Genion tool of GROMACS before switching to energy minimization. 1 ns NPT coordinates followed by 1 ns NVT coordinates were balanced during balancing while maintaining a steady 1 atm pressure and 300 K temperature. The created performance file is 'md 0 10.gro'. Using the GROMACS tool, the gro file was translated from 'md 0 10.gro' to 'md 0 10.pdb'. In addition, except for traces in the text editor, solutions were removed and the save file was revised. In the case of protein-protein interaction data accumulation, the pdb file was used for PIC and PILP.

2.2 Analysis of binding mode of BRI1 PRR with PAMP Brassinolide and Co-receptor SERk1

The intermolecular interactions amongst BRI1 PRR, PAMP Brassinolide (BLD) and SERk1 co-receptor have been formed in the complex using Chimera, a molecular visualization scheme. Using the Protein-Ligand Interaction Profiler (PLIP) and PIC instrument, H-bonds, hydrophobic interactions, ionic interactions, aromatic interactions and cation-Pi interactions were evaluated (Protein Interactions Calculator). For the structural complex, before and after the simulation, any kind of analysis was performed. Using the g_mmpbsa instrument, binding free energy calculations have been performed.

Chapter 3

Result and Discussion

Linkages between BRI1 with BLD as well as SERk1 were reviewed throughout this segment with the help of both Protein interaction calculation (PIC) and Protein-Ligand Interaction Profiler (PLIP). Furthermore, for better understanding, data found from hydrogen bond (h-bond), radius of Gyration (Rg) and root-mean-square deviation (RMSD) were also analyzed with proper graphs and figures.

3.1 H-Bond

Distribution of hydrogen bonds for protein-protein parameters throughout a simulation period of 5ns was computed. In the process, the protein-protein hydrogen bonds represent the elevating graph of the whole turn. It was intended to measure the configuration of the complete hydrogen bond at a distinctive period of time to fully comprehend the establishment of the hydrogen bond within two protein indexed databases. Figure 3A reveals that an estimation of 6 hydrogen bonds within BRI1 and BLD are positioned at 1300ps, whereas SERK1 is involved and an upper limit of 10 hydrogen bonds are formulated at 2400ps and 3000ps in the exclusion of SERK1. Here, Protein Interaction Calculation (PIC) as well as Protein Ligand Interaction Profiler (PLIP) findings have also shown that there is quite a few persistent hydrogen bonding among BRI1 and BLD, along with somewhat high proportion of hydrogen bond interactions within BRI1 and SERK1 which are stable.

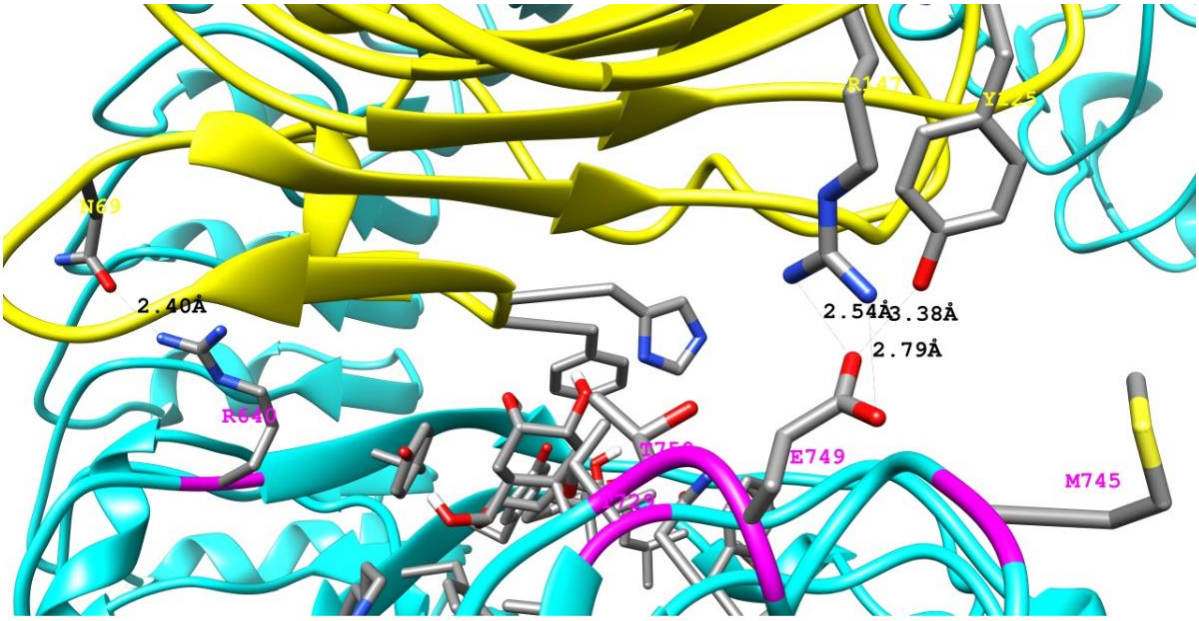

Fig 3.1.1: Cartoon structural view of prominent residues for interacting between BRI1 and SERK1 during the presence of BLD and there the interaction distance is calculated for H-bond.

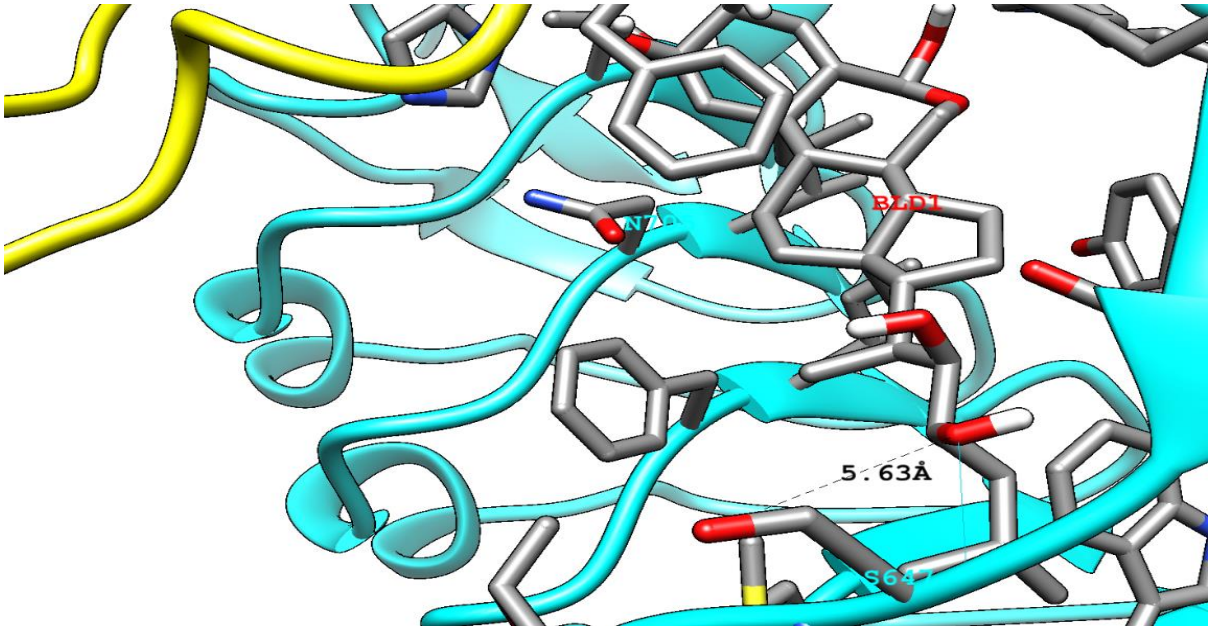

Fig 3.1.2: Cartoon structural view of prominent residues for interacting between BRI1 and BLD during the presence of Co-receptor SERk1 where the interaction distance is calculated for H- bond.

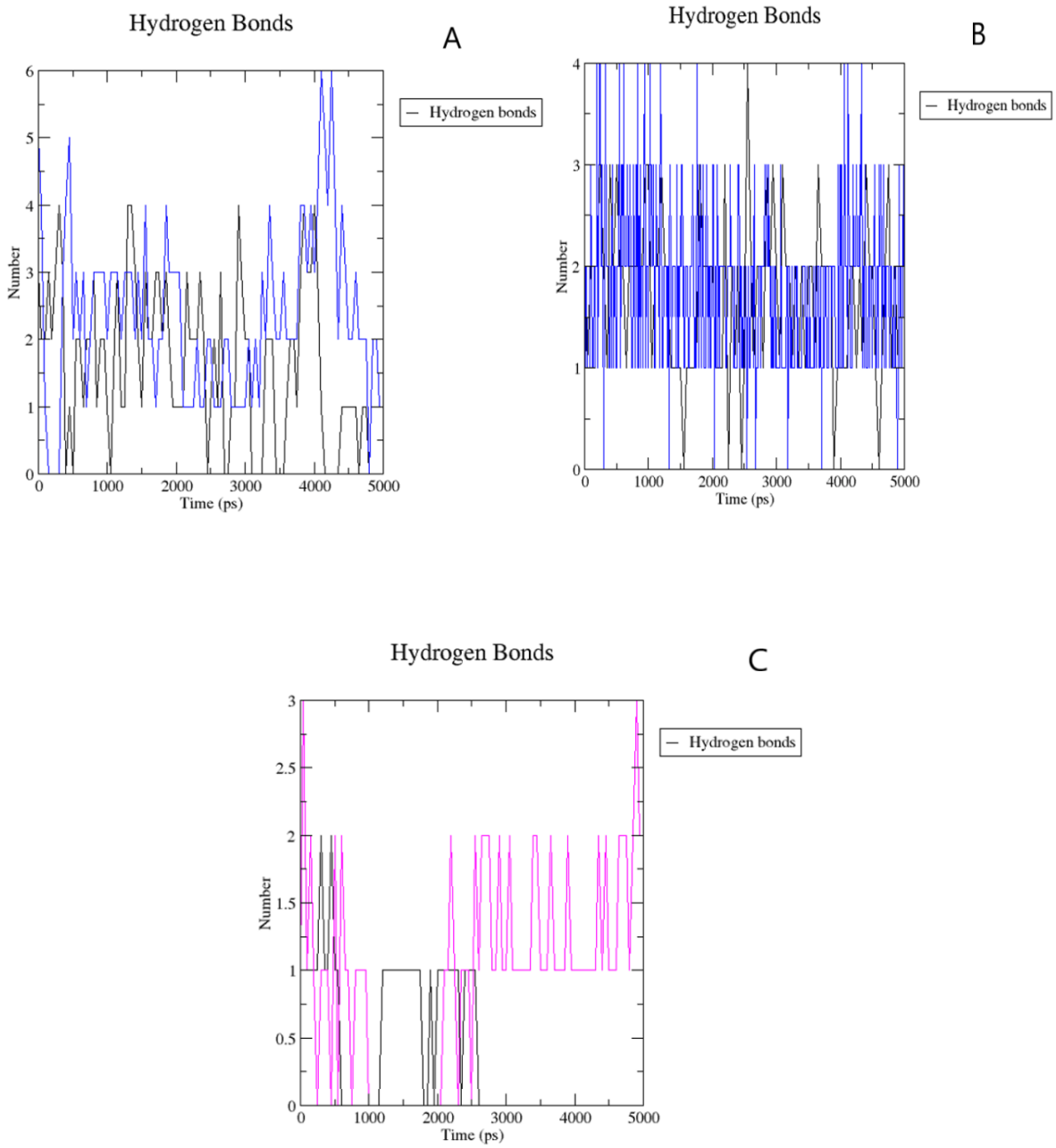

Fig 3.3.1: (A) H-bond value of BRI1 and BLD from 5ns MD trajectories. BRI1, BLD complex (Blue) presence of SERk1 in the complex, BRI1 and BLD complex (Black) absence of SERk1. **(B)** H-bond value of BRI1 and SERk1 from 5ns MD trajectories. BRI1, SERk1 complex (Blue) in the presence of BLD, BRI1 and SERk1 complex (Black) absence of BLD. **(C)** H-bond value of BLD and SERk1 from 5ns MD trajectories. BLD and SERk1 complex, BLD and SERk1 complex (Pink) presence of BRI1, BLD and SERk1 complex (Black) absence of BRI1.

3.2 Protein-Ligand Interaction Profiler (PLIP)

Table 3.2.1: Protein-Ligand Hydrophobic Interactions of BRI1-BLD-SERk1 complex before and after simulation.

Before Simulation					
Position	**Residue**	**Chain**	**Position**	**Residue**	**Chain**
564	TRP	A	1	BLD	A
564	TRP	A	1	BLD	A
597	TYR	A	1	BLD	A
599	TYR	A	1	BLD	A
682	ILE	A	1	BLD	A
705	ASN	A	1	BLD	A
After Simulation					
Position	**Residue**	**Chain**	**Position**	**Residue**	**Chain**
61	PHE	B	771	BLD	C
563	ILE	A	771	BLD	C
599	TYR	A	771	BLD	C
681	THE	A	771	BLD	C
705	ASN	A	771	BLD	C

Table 3.2.2: Protein-Ligand Hydrogen Interactions of BRI1-BLD-SERk1 complex before and after simulation.

Before Simulation					
Position	**Residue**	**Chain**	**Position**	**Residue**	**Chain**
62	HIS	C	1	BLD	A
597	TYR	A	1	BLD	A
642	TYR	A	1	BLD	A
642	TYR	A	1	BLD	A
647	SER	A	1	BLD	A

After Simulation					
Position	**Residue**	**Chain**	**Position**	**Residue**	**Chain**
62	HIS	B	771	BLD	C
597	TYR	A	771	BLD	C
597	TYR	A	771	BLD	C
642	TYR	A	771	BLD	C
647	SER	A	771	BLD	C
647	SER	A	771	BLD	C

Table 3.2.3: Protein-Ligand Hydrophobic Interactions of BRI1-BLD complex before and after simulation.

Before Simulation					
Position	**Residue**	**Chain**	**Position**	**Residue**	**Chain**
564	TRP	A	1	BLD	A
564	TRP	A	1	BLD	A
597	TYR	A	1	BLD	A
599	TYR	A	1	BLD	A
682	ILE	A	1	BLD	A
705	ASN	A	1	BLD	A
After Simulation					
Position	**Residue**	**Chain**	**Position**	**Residue**	**Chain**
599	TYR	A	771	BLD	B
646	THR	A	771	BLD	B
648	PRO	A	771	BLD	B
705	ASN	A	771	BLD	B

Table 3.2.4: Protein-Ligand Hydrogen Interactions of BRI1-BLD complex before and after simulation.

Before Simulation					
Position	**Residue**	**Chain**	**Position**	**Residue**	**Chain**
597	TYR	A	1	BLD	A
642	TYR	A	1	BLD	A
642	TYR	A	1	BLD	A
647	SER	A	1	BLD	A
After Simulation					
Position	**Residue**	**Chain**	**Position**	**Residue**	**Chain**
597	TYR	A	771	BLD	B
597	TYR	A	771	BLD	B
647	SER	A	771	BLD	B

Table 3.2.5: Protein-Ligand Hydrophobic Interactions of SERK1-BLD complex before and after simulation.

Before Simulation					
No Interaction Found					
After Simulation					
Position	**Residue**	**Chain**	**Position**	**Residue**	**Chain**
61	PHE	A	212	BLD	B
61	PHE	A	212	BLD	B
61	PHE	A	212	BLD	B
61	PHE	A	212	BLD	B

Table 3.2.6: Protein-Ligand Hydrogen Interactions of SERK1-BLD complex before and after simulation.

Before Simulation					
Position	**Residue**	**Chain**	**Position**	**Residue**	**Chain**
62	HIS	C	1	BLD	A
After Simulation					
Position	**Residue**	**Chain**	**Position**	**Residue**	**Chain**
63	VAL	A	212	BLD	B

3.3 Protein Interactions Calculator (PIC)

Table 3.3.1: Protein-Protein Hydrophobic Interactions of BRI1-SERK1 complex.

Position	Residue	Chain	Position	Residue	Chain
642	TYR	A	61	PHE	C
765	TYR	A	145	PHE	C

NO PROTEIN-PROTEIN DISULPHIDE BRIDGES FOUND

Table 3.3.2: Protein-Protein Main Chain-Main Chain Hydrogen Bonds of BRI1-SERK1 complex.

DONOR				**ACCEPTOR**				
POS	**CHAIN**	**RES**	**ATOM**	**POS**	**CHAIN**	**RES**	**ATOM**	**Dd-a**
640	A	ARG	NH2	69	C	ASN	OD1	2.40
640	A	ARG	NH2	69	C	ASN	OD1	2.40
726	A	THR	OG1	78	C	ASN	OD1	3.03

747	A	GLN	NE2	101	C	TYR	OH	2.63
747	A	GLN	NE2	101	C	TYR	OH	2.63
62	C	HIS	NE2	727	A	MET	SD	3.71
78	C	ASN	OD1	726	A	THR	OG1	3.03
78	C	ASN	OD1	726	A	THR	OG1	3.03
101	C	TYR	OH	747	A	GLN	NE2	2.63
125	C	TYR	OH	749	A	GLU	OE2	3.38
147	C	ARG	NH1	749	A	GLU	OE1	2.79
147	C	ARG	NH1	749	A	GLU	OE1	2.79
147	C	ARG	NH1	749	A	GLU	OE2	2.95
147	C	ARG	NH1	749	A	GLU	OE2	2.95
147	C	ARG	NH2	749	A	GLU	OE2	2.54
147	C	ARG	NH2	749	A	GLU	OE2	2.54

Table 3.3.3: Protein-Protein Ionic Interactions of BRI1-SERk1 complex.

Protein-Protein Ionic Interactions					
Position	**Residue**	**Chain**	**Position**	**Residue**	**Chain**
702	ARG	A	80	GLU	C
749	GLU	A	147	ARG	C

Table 3.3.4: Protein-Protein Aromatic interaction of BRI1-SERk1 complex.

PROTEIN-PROTEIN AROMATIC-AROMATIC INTERACTIONS						
Position	**Residue**	**Chain**	**Position**	**Residue**	**Chain**	**D(centroid-centroid)**
642	TYR	A	61	PHE	C	6.91
765	TYR	A	145	PHE	C	6.24

3.4 Root Mean Square Deviation (RMSD)

The accuracy of the MD simulation was verified by assessing Root mean square deviation in the circumstances of deviations. The time shift of the RMSDs of BRI1, BLD and SERK1 (Just backbone) is accessed as a function of period. The RMSDs for BRI1, BLD and SERK1 in the three computerized implementations are shown in the **figure** 3.4.1 in addition where RMSD values from 5ns MD trajectories are given. The backbone of three proteins indicated variable RMSD in distinct simulated structures. A 3ns equilibrium is required for BRI1, BLD, and SERK1. Optimal deviations are 7.85nm and 8nm at 1ns and 3ns, respectively, before 3ns of the time period. Although the time graph dips briefly at 1.5ns(7.7nm) after equilibrium, it continues to step steadily forward with a standard deviation (SD) of 7.8nm. It has a reasonably stable position of 3ns and deviates between 7.85nm and 8nm until the end of the simulation. When SERK1 is not present in the complex, however, the BRI1 and BLD complex combinations are not as stable as they were previously. Rather, the graph shows rigidity right at the start of the simulation. After 2.5ns, the highest divergence remains, and after 3ns, it deviates at 8nm, which is considered the highest in that order. In this situation, there is also variability at 3ns, as seen by the high RMSDs between these periods. The RMSD of BRI1 and SERK1 is viewed in a related way. The complex's primary process, as previously said, is balanced and demonstrates equilibrium. It deviates to 7.75nm at 0.5ns and dramatically increases to 7.85nm after 1ns, while the RMSD exhibits marginal uniformity with a standard deviation of 7.75nm from 3ns to 3.5ns of the simulation, but stops before the end. As previously stated, an unstable variance is characterized in the same way that BRI1 and SEKR1 RMSD without BLD show instability in the sense of BRI1 and BLD RMSD without SERK1. Furthermore, as previously said, when SERK1 is present in the BRI1 and BLD RMSD complex, it exhibits 3ns stability; but, in this situation, it seems to be unstable from 3.5ns to the end of the simulation period. In all three examples, BRI1, BLD, and SERK1 RMSD are found to be more stable when they are all within the complex and interact with one another. With SERK1, BRI1 RMSD, and BLD deviating more and more, another situation is shown to be disorganized. As a result, SERK1 must really be functional for BRI1 to associate with BLD.

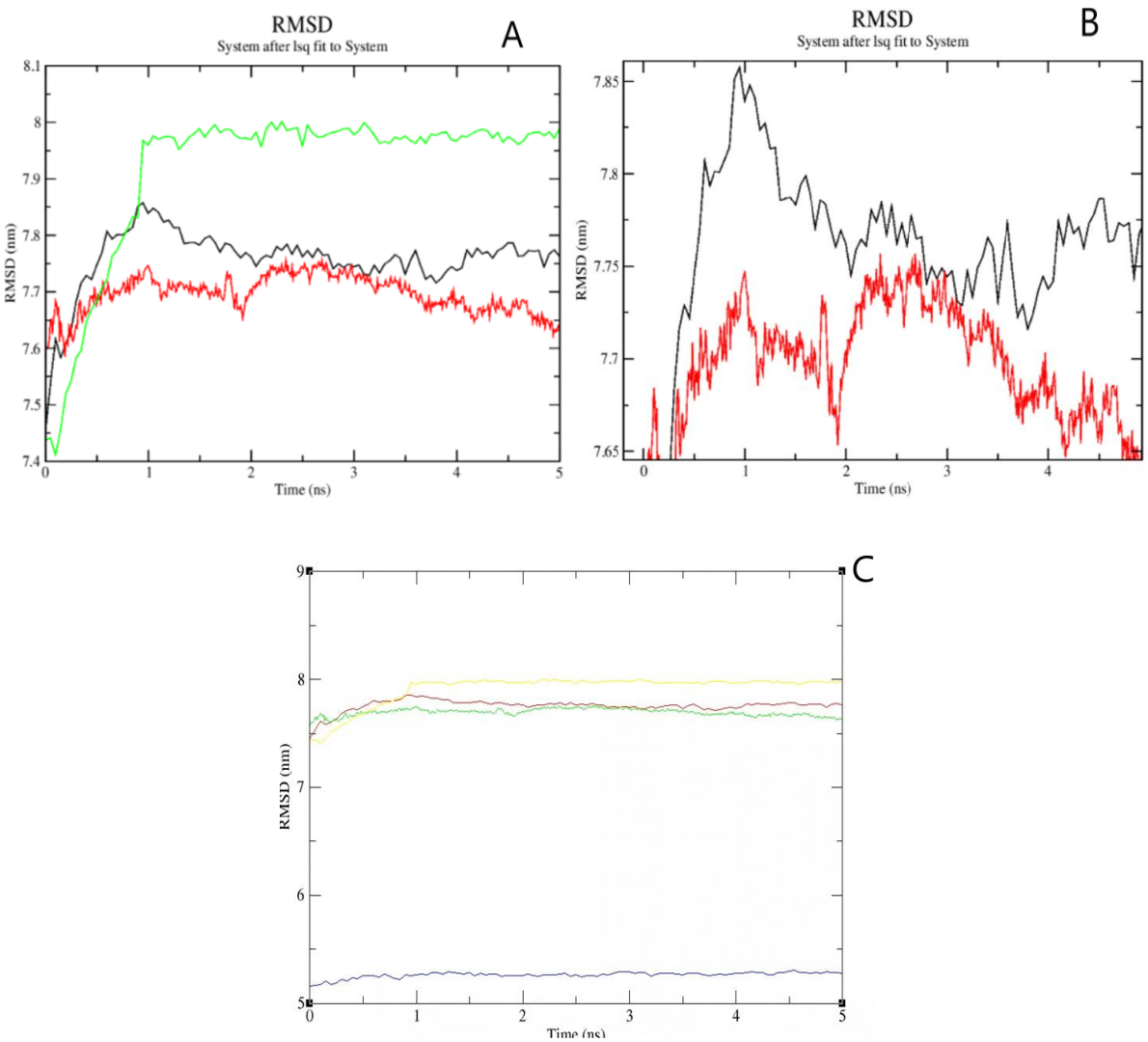

Fig 3.4.1: (A) Comparison of RMSD value of BRI1-BLD-SERk1 complex (Black), BRI1-BLD complex (red) and BRI1-SERk1 complex (green). **(B)** Comparison of RMSD value of BRI1-BLD-SERk1 complex (Black) and BRI1-BLD complex (red). (**C**) Comparison of RMSD value of the BRI1-BLD-SERk1 complex (yellow), BRI1-BLD complex (red), BRI1-SERk1 complex (green) and BLD-SERk1 (blue).

3.5 Radius of Gyration

Gyration radius (Rg) values are calculated to determine the uniformity of all structures. Furthermore, in direct comparison to the BRI1-BLD-SERK1 complex as well as the BRI1-SERK1 complex, the BRI1-BLD Rg complex has somewhat fluctuated. This tendency is most evident in the 3000ps of the simulation, when the BRI1 BLD complex extends to a peak value of approximately 5.43 nm throughout the first 2000ps and then drops to a low value of about 5.415 nm near the 2500ps mark. The graph appears somewhat compatible with the BRI1-BLD-SERK1 complex in this time period. At the same time, BLD-SERK1 complexes are prone to a variety of instabilities. Though it reaches 5.425nm at 500ps, it then drops to 5.375nm at 1000ps. More changes in the Rg values are reflected by a further changing structure, which again is persistent with higher deviations in the BRI1-SERK1 complex and BRI1-BLD complex; because, proteins are prone to uncoiling and recoiling on their own. SERK1, on the other hand, interacts with BRI1 and BLD in a single complex, it is step restricted but less vulnerable to uncoiling, resulting in a graph that is less fluctuating.

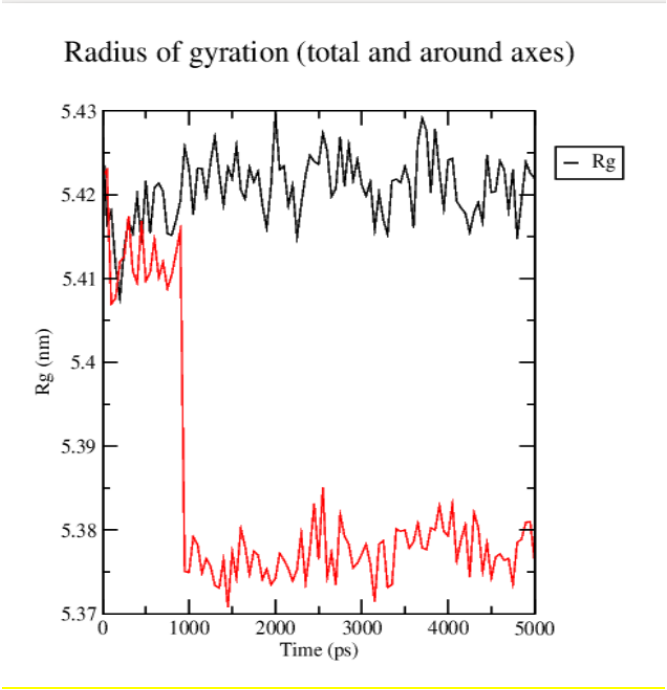

Fig 3.5.1: Rg value from 5ns MD trajectories. Rg of BRI1 and BLD when SERk1 is present in the complex (Black). Rg of BRI1 and SERK1 when BLD is absent in the complex (Red).

3.6 Discussion

A plant PRR computational evaluation was identified and assessed for the association between PRR RLK BRI1 and PAMP BLD and Coreceptor SERk1. All things considered; the results demonstrate the activation procedure for a plant LRR receptor kinase wherein an integral part of the receptor ligand binding region is formed by a sort of analogous co receptor protein. As it has been already demonstrated that how the complex structure of BRI1-BLD-SERK1 indicates that BLD acts as a "molecular glue" that facilitates the receptor's interaction with its co-receptor, which allows their kinase domains to engage and ultimately activate the signaling pathway. (37) The extensive utilization of multifunctional SERKs in plant membrane signaling may enable cross signaling explicitly only at cell surface layer of ligand sensing and also can instigate the sensitivity of the plant to exterior triggers. [38]. Furthermore, in the island domain β sheet (Tyr597, Tyr599, and Tyr642), which itself is portion of the hormone attachment region, Glu643 in BRI1 leads to a hydrogen-bonded scheme. The BRI1-BLD structure illustrates that ligand-independent BRI1 does not signal, but instead adjusts the receptor's hormone-bound phase. Polar correlations between both the Arg596 island domain and the mainchain oxygen and nitrogen from Ile621 also occurred throughout the engagement. Besides that, Glu643's subsequent contacts in BRI1 to Ser623 and Glu624 were modulated by a water molecule at the phase of complex formulation.

Besides, a thorough study of BLD and BRI1 LRR domain interconnections confirms that despite the absence of SERK1 in the complex, Ser647 from BRI1 still interacts favorably with BLD, however other residues in the SERK1 affiliation show suitable connection. It is observed from BLD engagement that in the presence of SERK1, the 2α-3α-diol component of BLD is more favorable. Further, from the interpretation of data from H-bond, Protein-Ligand Interaction Profiler (PLIP) and Protein Interaction Calculation (PIC), it is demonstrated that in addition to hydrogen bond, initially explained suitable residues have a number of interactions. For more scrutinization, cross check is facilitated among prior researched crystallographic structures as well as the BRI1-BLD-SERk1 complex. In order to interact with LRR-RKs and peptide hormones, certain protocols are pursued typically.

Chapter 4

Conclusions and Recommendations

4.1 Conclusions

From the study of 5ns of BRI1, BLD and SERk1 complex trajectories using RMSD, H-bond, PLIP and PIC it could be said co-receptor SERk1 should be present within the complex for immune response to BLD. While it is found from 5ns RMSD trajectories that even after 5ns the entire complex appears to be stable, if the simulation time is extended to 30ns, 50 ns or 100ns, more consistency can be found. In addition, the significant residues discovered by analysing data from the 5ns trajectories. If in the future the simulation time is extended, more prominent residues can be obtained again, the observed prominent residues obtained from 5ns trajectories can be checked whether or not they will remain prominent as before. There are significant variations observed in various types of interaction alongside H-bond from H-bond, PLIP and PIC outcome after 5ns simulation than before the simulation. The extended duration of simulation would indicate which kinds of interactions are more responsible and which interactions are less significant. But from 5ns trajectories, as it is observed, SERk1 co-receptor immune response performs a significant role, so it can be presumed that it will remain the same after the simulation time is extended.

4.1 Recommendations for Future Works

This research can be furthered by obtaining such standards, for example.

- This study could be improved by running the molecular dynamic simulation for a longer time (30ns or 50ns), which would allow for more specific and definitive results. It is possible to build a better understanding of protein character.
- MM/PBSA, may be applied that is a post-processing method wherein the free energy of a state is determined from the internal energy (MM) of the residues and its linkage with a clear and understandable representation of solvent (PBSA).

- This study may be useful for the interrelationships of BRI1 LRR and other mutated PAMPs in the *Arabidopsis thaliana* plant. The profound relationship of the PRR-PAMP complex, and also the intervention of the mutated coreceptor, will show how a mutant molecule can induce changes in particular residues and interactions, resulting in pattern triggered immunity (PTI).

References

1. Resjö, S., Zahid, M.A., Burra, D.D., Lenman, M., Levander, F., and Andreasson, E., 2019. *Proteomics of PTI and Two ETI Immune Reactions in Potato Leaves*. *International Journal of Molecular Sciences*, 20 (19), 4726.
2. Laibach, F. 1 943. *Arabidopsis thaliana (L.) Heynh. als Objekt fiir genetische und entwickIungsphysiologische Untersuchungen.* Bot. Archiv. 44:439-55
3. Redei, G. P. 1975. *Arabidopsis as a genetic tool.* Ann. Rev. Genet. 9: 1 1 1-27
4. Leutwiler, L. S., 1984. *The DNA of Arabidopsis thaliana.* Mol. Gen. Genet. 1 94: 1 5-23
5. Meyerowitz EM, Chang C. *Molecular biology of plant growth and development. Arabidopsis thaliana as an experimental system*. Dev Biol (N Y 1985). 1988; 5:353-66.
6. Shindo, C., Bernasconi, G., & Hardtke, C. S. (2007). *Natural Genetic Variation in Arabidopsis: Tools, Traits and Prospects for Evolutionary Ecology*. Annals of Botany, *99*, 1043–1054.
7. Meyerowitz EM. *Arabidopsis thaliana.* Annu Rev Genet. 1987; 21:93-111.
8. Zhou, J., Liu, D., Wang, P., Ma, X., Lin, W., Chen, S., … Shan, L. (2018). Regulation of Arabidopsis brassinosteroid receptor BRI1 endocytosis and degradation by plant U-box PUB12/PUB13-mediated ubiquitination. *Proceedings of the National Academy of Sciences*, *115*, E1906–E1915.
9. Li, J., & Chory, J.. (1997). *A Putative Leucine-Rich Repeat Receptor Kinase Involved in Brassinosteroid Signal Transduction*. *Cell*, *90*, 929–938.
10. Ogawa M, Shinohara H, Sakagami Y, Matsubayashi Y. *Arabidopsis CLV3 peptide directly binds CLV1 ectodomain*. Science. 2008 Jan 18;319(5861):294.
11. Gómez-Gómez L, Boller T. *FLS2: an LRR receptor-like kinase involved in the perception of the bacterial elicitor flagellin in Arabidopsis.* Mol Cell. 2000 Jun;5(6):1003-11.
12. Wang, Z.-Y., Bai, M.-Y., Oh, E., & Zhu, J.-Y. (2012). *Brassinosteroid Signaling Network and Regulation of Photomorphogenesis. Annual Review of Genetics, 46*(1), 701-724.
13. He, Z.. (2000). *Perception of Brassinosteroids by the Extracellular Domain of the Receptor Kinase BRI1*. *Science*, *288*, 2360–2363.
14. Kinoshita, T., Caño-Delgado, A., Seto, H. *et al. Binding of brassinosteroids to the extracellular domain of plant receptor kinase BRI1*. *Nature* **433,** 167–171 (2005).
15. She, J., Han, Z., Kim, TW. *et al. Structural insight into brassinosteroid perception by BRI1*. *Nature* **474,** 472–476 (2011).
16. Hothorn, M., Belkhadir, Y., Dreux, M. *et al. Structural basis of steroid hormone perception by the receptor kinase BRI1*. *Nature* **474,** 467–471 (2011).
17. Li, J., Wen, J., Lease, K. A., Doke, J. T., Tax, F. E., & Walker, J. C.. (2002). *BAK1, an Arabidopsis LRR Receptor-like Protein Kinase, Interacts with BRI1 and Modulates Brassinosteroid Signaling*. *Cell*, *110*, 213–222.

18. Nam, K. H., & Li, J. (2002). *BRI1/BAK1, a Receptor Kinase Pair Mediating Brassinosteroid Signaling*. *Cell*, *110*, 203–212.
19. Gou X, Yin H, He K, Du J, Yi J, et al. (2012) Genetic Evidence for an Indispensable Role of Somatic Embryogenesis Receptor Kinases in Brassinosteroid Signaling. PLOS
20. Karlova, R., Boeren, S., Russinova, E., Aker, J., Vervoort, J., & De Vries, S. (2006). The Arabidopsis SOMATIC EMBRYOGENESIS RECEPTOR-LIKE KINASE1 Protein Complex Includes BRASSINOSTEROID-INSENSITIVE1. *The Plant Cell*, *18*, 626–638.
21. Mesirov, J. P., Schulten, K., & L., S. D. (1996). *Mathematical approaches to biomolecular structure and dynamics*. New York: Springer.
22. Salentin, S., Schreiber, S., Haupt, V. J., Adasme, M. F., & Schroeder, M. (2015). *PLIP: fully automated protein–ligand interaction profiler*. *Nucleic Acids Research*, *43*, W443–W447.
23. Tina, K. G., Bhadra, R., & Srinivasan, N.. (2007). *PIC: Protein Interactions Calculator*. *Nucleic Acids Research*, *35*, W473–W476.
24. Genheden, S., & Ryde, U.. (2015). *The MM/PBSA and MM/GBSA methods to estimate ligand-binding affinities. Expert Opinion on Drug Discovery*, *10*, 449–461.
25. Connolly, M.. (1983). Solvent-accessible surfaces of proteins and nucleic acids. *Science*, *221*, 709–713.
26. Lee B, Richards FM. *The interpretation of protein structures: estimation of static accessibility*. J Mol Biol. 1971 Feb 14;55(3):379-400.
27. Richards, F. M. (1977). *AREAS, VOLUMES, PACKING, AND PROTEIN STRUCTURE. Annual Review of Biophysics and Bioengineering, 6*(1), 151-176. doi:10.1146/annurev.bb.06.060177.001055
28. Greer, J., & Bush, B. L. (1978). *Macromolecular shape and surface maps by solvent exclusion*. *Proceedings of the National Academy of Sciences of the United States of America*, *75*(1), 303–307.
29. Jiang, F., & Kim, S.-H. (1991). *"Soft docking": Matching of molecular surface cubes*. *Journal of Molecular Biology*, *219*(1), 79-102.
30. Shrake, A., & Rupley, J. A. (1973). *Environment and exposure to solvent of protein atoms. Lysozyme and insulin. Journal of Molecular Biology, 79*(2), 351-371.
31. Shrake, A. *Environment and exposure to solvent of protein atoms. Lysozyme and insulin. Journal of Molecular Biology, 79*(2), 351-371.
32. Huggins, M. L. (1971). 50 Years of Hydrogen Bond Theory. *Angewandte Chemie International Edition in English, 10*(3), 147-152.
33. McDonald, I. K., & Thornton, J. M. (1994). *Satisfying Hydrogen Bonding Potential in Proteins. Journal of Molecular Biology, 238*(5), 777-793.

34. Creighton, T. E. (1991). *Stability of folded conformations: Current opinion in structural biology* 1991, 1: 5–16. *Current Opinion in Structural Biology*, *1*(1), 5-16. Dill, K. A. (1990). *Dominant forces in protein folding*. *Biochemistry*, *29*(31), 7133-7155.
35. Van Der Spoel, D., Lindahl, E., Hess, B., Groenhof, G., Mark, A. E., & Berendsen, H. J. C. (2005). *GROMACS: Fast, flexible, and free. Journal of Computational Chemistry*, *26*(16), 1701-1718.
36. Van Der Spoel, D., Van Maaren, P. J., & Berendsen, H. J. C.. (1998). *A systematic study of water models for molecular simulation: Derivation of water models optimised for use with a reaction field*. *The Journal of Chemical Physics*, *108*, 10220–10230.
37. Wang, X., Kota, U., He, K., Blackburn, K., Li, J., Goshe, M. B., . . . Clouse, S. D. (2008). *Sequential Transphosphorylation of the BRI1/BAK1 Receptor Kinase Complex Impacts Early Events in Brassinosteroid Signaling. Developmental Cell*, *15*(2), 220-235.
38. Belkhadir, Y., Jaillais, Y., Epple, P., Balsemao-Pires, E., Dangl, J. L., & Chory, J.. (2012). *Brassinosteroids modulate the efficiency of plant immune responses to microbe-associated molecular patterns. Proceedings of the National Academy of Sciences*, *109*, 297–302.
39. Moreno-Castillo, E., Ramírez-Echemendía, D. P., Hernández-Campoalegre, G., Mesa-Tejeda, D., Coll-Manchado, F., & Coll-García, Y. (2018*). In silico identification of new potentially active brassinosteroid analogues*. *Steroids, 138*, 35-42.
40. Zhu, J.-Y., Sae-Seaw, J., & Wang, Z.-Y.. (2013). *Brassinosteroid signalling*. *Development*, *140*, 1615–1620.
41. Belkhadir, Y., & Jaillais, Y.. (2015). *The molecular circuitry of brassinosteroid signaling*. *New Phytologist*, *206*, 522–540.
42. Lei, B., Liu, J., & Yao, X. (2015). *Unveiling the molecular mechanism of brassinosteroids: Insights from structure-based molecular modeling studies. Steroids, 104*, 111-117.
43. Han, Z., Sun, Y., & Chai, J. (2014). *Structural insight into the activation of plant receptor kinases*. *Current Opinion in Plant Biology*, *20*, 55-63.
44. Sun, Y., Han, Z., Tang, J., Hu, Z., Chai, C., Zhou, B., & Chai, J.. (2013). *Structure reveals that BAK1 as a co-receptor recognises the BRI1-bound brassinolide*. *Cell Research*, *23*, 1326–1329.

45. Wang, Z.-Y., Seto, H., Fujioka, S., Yoshida, S., & Chory, J. (2001). *BRI1 is a critical component of a plasma-membrane receptor for plant steroids. Nature, 410*(6826), 380-383.
46. She, J., Han, Z., Kim, T.-W., Wang, J., Cheng, W., Chang, J., … Chai, J.. (2011). *Structural insight into brassinosteroid perception by BRI1*. *Nature*, *474*, 472–476.
47. Friedrichsen, D. M., Joazeiro, C. A. P., Li, J., Hunter, T., & Chory, J.. (2000). *Brassinosteroid-Insensitive-1 Is a Ubiquitously Expressed Leucine-Rich Repeat Receptor Serine/Threonine Kinase*. *Plant Physiology*, *123*, 1247–1256.

48. Hothorn, M., Belkhadir, Y., Dreux, M., Dabi, T., Noel, J. P., Wilson, I. A., & Chory, J.. (2011). *Structural basis of steroid hormone perception by the receptor kinase BRI1*. *Nature*, *474*, 467–471.
49. Shiu, S.-H., & Bleecker, A. B.. (2001). *Receptor-like kinases from Arabidopsis form a monophyletic gene family related to animal receptor kinases*. *Proceedings of the National Academy of Sciences*, *98*, 10763–10768.

Appendixes.

A number of bioinformatics tools were used in this study. For instance,

Tool	Purpose
Protein interactions calculator: PIC (online)	Residual bond identification
The Protein-Ligand Interaction Profiler	Identification of non-covalent interactions
Chimera	Molecular visualization
xmgrace	Graph generation and analysis